Article

Cell Reports

A CREB-Sirt1-Hes1 Circuitry Mediates Neural Stem Cell Response to Glucose Availability

Graphical Abstract

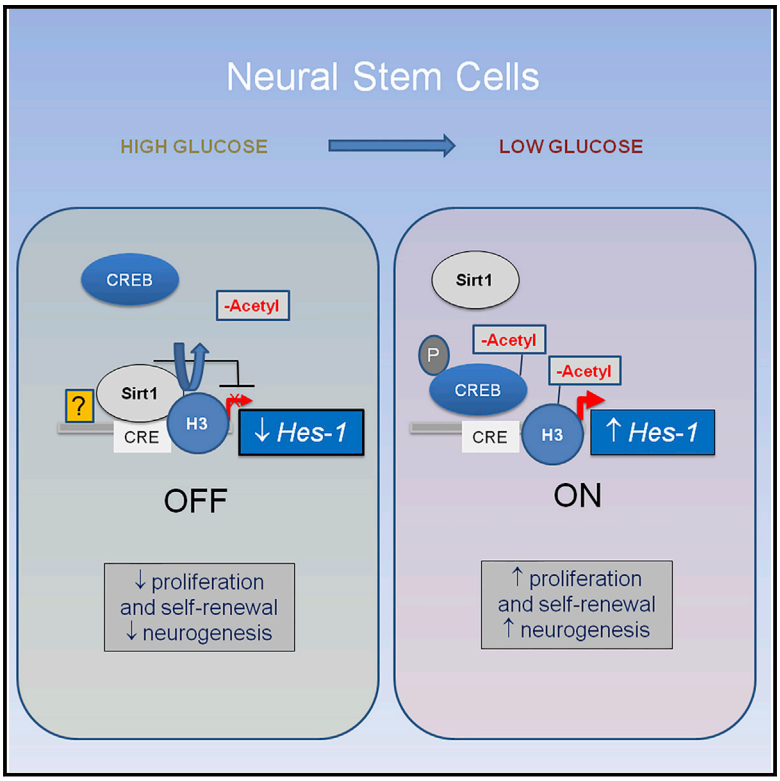

Authors

Salvatore Fusco, Lucia Leone, Saviana Antonella Barbati, ..., Michael McBurney, Giovambattista Pani, Claudio Grassi

Correspondence

gpani@rm.unicatt.it

In Brief

Using a combination of in vitro and in vivo studies, Fusco et al. find that excess glucose impairs the self-renewal capacity of neural stem cells through a molecular circuit that involves the transcription factor CREB and Sirtuin 1. The authors suggest that this circuitry may link nutrient excess with neurodegeneration and brain aging.

Highlights

- Low glucose promotes NSC proliferation and self-renewal in vitro
- Glucose regulates *Hes-1* expression through a CREB-Sirt1 metabolic switch
- Calorie restriction triggers the CREB-Sirt1-*Hes1* switch in the hippocampus of mice
- This circuitry may link nutrient excess with neurodegeneration and brain aging

Fusco et al., 2016, Cell Reports *14*, 1195–1205
February 9, 2016
http://dx.doi.org/10.1016/j.celrep.2015.12.092

Cell Reports
Article

A CREB-Sirt1-Hes1 Circuitry Mediates Neural Stem Cell Response to Glucose Availability

Salvatore Fusco,[1,6,7] Lucia Leone,[1,7] Saviana Antonella Barbati,[1] Daniela Samengo,[2] Roberto Piacentini,[1] Giuseppe Maulucci,[3] Gabriele Toietta,[4] Matteo Spinelli,[1] Michael McBurney,[5] Giovambattista Pani,[2,*] and Claudio Grassi[1,6]

[1]Institute of Human Physiology
[2]Institute of General Pathology
[3]Institute of Physics
Università Cattolica Medical School, 00168 Rome, Italy
[4]Regina Elena National Cancer Institute, 00144 Rome, Italy
[5]Centre for Cancer Therapeutics, Ottawa Hospital Research Institute, Ottawa, ON 81H KL6, Canada
[6]San Raffaele Pisana Scientific Institute for Research, Hospitalization and Health Care, 00163 Rome, Italy
[7]Co-first author
*Correspondence: gpani@rm.unicatt.it
http://dx.doi.org/10.1016/j.celrep.2015.12.092

SUMMARY

Adult neurogenesis plays increasingly recognized roles in brain homeostasis and repair and is profoundly affected by energy balance and nutrients. We found that the expression of *Hes-1* (hairy and enhancer of split 1) is modulated in neural stem and progenitor cells (NSCs) by extracellular glucose through the coordinated action of CREB (cyclic AMP responsive element binding protein) and Sirt-1 (Sirtuin 1), two cellular nutrient sensors. Excess glucose reduced CREB-activated *Hes-1* expression and results in impaired cell proliferation. CREB-deficient NSCs expanded poorly in vitro and did not respond to glucose availability. Elevated glucose also promoted Sirt-1-dependent repression of the *Hes-1* promoter. Conversely, in low glucose, CREB replaced Sirt-1 on the chromatin associated with the *Hes-1* promoter enhancing Hes-1 expression and cell proliferation. Thus, the glucose-regulated antagonism between CREB and Sirt-1 for Hes-1 transcription participates in the metabolic regulation of neurogenesis.

INTRODUCTION

Metabolic imbalance associated with obesity and diabetes negatively affects cognitive function, increases the risk for degenerative diseases, and accelerates brain aging through molecular and cellular mechanisms that are still incompletely understood (Cukierman et al., 2005; Messier, 2005). Beside targeting adult neuronal networks and brain vasculature, conditions such as hyperglycemia and dyslipidemia are suspected of affecting adult neurogenesis by reducing the number and function of neural stem and progenitor cells (NSCs) (Park and Lee, 2011).

Adult neurogenesis (i.e., generation of new neurons throughout life) occurs in specialized areas of the mammalian brain including the dentate gyrus (DG) of the hippocampus, where NSCs reside and participate in brain functions including learning, memory, and damage repair (Gage, 2000; Zhang et al., 2008). A delicate balance is maintained between NSC self-renewal and commitment to differentiation along multiple (neuronal, astrocytic, and oligodendrocytic) lineages. The *Notch* signaling pathway—through its downstream effectors, the basic helix-loop-helix transcriptional regulators *Hes-1* and *Hes-5* (hairy and enhancer of split 1 and 5)—appears to promote NSC self-renewal (Ohtsuka et al., 2001), while signaling through the epidermal growth factor receptor seems to facilitate asymmetric division and lineage commitment (Aguirre et al., 2010). A decline in neurogenesis accompanies brain aging (Bondolfi et al., 2004) and may have a role in age-related neurodegenerative disorders (Mattson, 2000).

Adult neurogenesis is responsive to several environmental cues, including energy intake and nutrient availability (Rafalski and Brunet, 2011), highlighting the emerging connection between metabolic and brain diseases. Under conditions of high energy supply, NSC commitment toward progenitor elements (transit amplifying cells) increases at the expense of self-renewal, resulting in a reduced NSC pool. These events are controlled by the mammalian target of rapamycin (mTOR) serine-threonine kinase (Magri et al., 2011) and the starvation-activated transcription factor FoxO3A (Renault et al., 2009). Consistent with these findings, reduced hippocampal NSC proliferation, or a transiently increased progenitor expansion followed by defective maturation into adult neurons, has been reported in rodent models of diabetes (Saharan et al., 2013; Lang et al., 2009), whereas calorie restriction (CR) improves brain function and cognitive performance in mice, at least in part, by preserving and enhancing adult neurogenesis (Mattson, 2000; Park and Lee, 2011).

We have recently shown that the cyclic AMP responsive element binding protein (CREB) transcription factor is activated by nutrient deprivation in adult neurons and mediates the improved cognitive, electrophysiological, and pro-survival effects of low calorie intake (Fusco et al., 2012b). This action involves the protein deacetylase Sirtuin 1 (Sirt-1), an evolutionarily conserved nutrient sensor and longevity protein shown to have neuroprotective properties (Qin et al., 2006). Both Sirt-1 (Hisahara et al., 2008; Prozorovski et al., 2008) and CREB (Dworkin et al., 2009; Nakagawa et al., 2002) participate in adult neurogenesis, and CREB in particular may have a role in neurogenesis modulation by antidepressant drugs (Gur et al., 2007). Whether a CREB-Sirt1 signaling axis is also involved in nutrient sensing by NSCs and, by extension, in the metabolic regulation of neurogenesis is still unknown. We describe here a nutrient-signaling circuitry involving the coordinated action of CREB and Sirt-1 that regulates *Hes-1* expression and NSC self-renewal and expansion in vitro. We also show that the same glucose-sensing circuitry is activated in the hippocampus of mice subject to CR, resulting in enhanced NSC proliferation.

RESULTS

Ambient Glucose Affects NSC Self-Renewing Capacity In Vitro

NSCs isolated from mouse hippocampus can be expanded in vitro to generate clonal aggregates called neurospheres (NSs) (Reynolds and Weiss, 1992). NSs comprise a mixture of true stem elements and more committed progenitors, and their number and size provide reliable estimates of stem cell number and renewal capacity (neurosphere assay, NSA) (Deleyrolle et al., 2011; Kippin et al., 2005). To model the effect of excess glucose on neurogenesis, we performed NSA by reseeding disaggregated NSs from newborn C57BL/6 mouse hippocampi into culture media containing either 4.5 g/L (25 mM) or 1.0 g/L (5 mM) glucose. Although most media formulations recommend high glucose concentrations for NSC expansion, nearly twice as many NSs were formed in 1.0 g/L glucose compared to 4.5 g/L glucose ($p < 0.001$) (Figure 1A). NSs formed in low glucose were larger (Figures S1A and S1B) and contained a higher proportion of proliferating cells as assessed by the incorporation of the thymidine analog bromodeoxyuridine (BrdU) (Figures 1B and 1C). Moreover, the percentage of cells brightly stained by a fluorescent reporter of ALDH activity ($ALDH^{br}$), a biochemical hallmark of stem cells from brain and other tissues (Corti et al., 2006), was higher in NSCs grown in low compared to high glucose (6.6% ± 2.5% versus 3.4% ± 1.6%, $p < 0.05$) (Figures 1D and 1E). In NSCs grown in low glucose, there was no adaptive increase of glucose transport and the glucose consumption rate was lower than in high glucose medium (Figures S1C and S1D). Instead, mRNA encoding subunit IV of mitochondrial cytochrome oxidase (COX IV) was higher in low-glucose NSs, consistent with enhanced mitochondrial respiration in low-glucose-grown cells (Figure S1F). Low glucose was accompanied by reduced levels of intracellular reactive oxygen species (ROS) (Figure S1E) and by lower levels of phosphorylation of multiple components of the insulin/mTOR/S6K signaling cascade (Figure S1G), two changes reportedly associated with lower oxidative damage and enhanced stem cell self-renewal (Ito et al., 2004; Jang and Sharkis, 2007). Finally, low-glucose NS cultures contained elevated levels of *Hes-1* mRNA and protein (Figures 1F and 1G), one of the known markers or determinants of NSC identity (Aguirre et al., 2010; Ohtsuka et al., 2001). Low glucose had no effect on the NS cell death rate in otherwise complete medium (<5% as assessed by propidium iodide exclusion) but promoted cell survival or expansion in the absence of exogenous growth factors (Figure S1H) (Panieri et al., 2010).

A cAMP-PKA-$pCREB^{Ser133}$-*Hes1* Cascade Mediates NSC Response to Glucose

We next asked whether the transcription factor CREB, as a nutrient detector in adult neurons (Fusco et al., 2012b), had a role in the observed NSC response to glucose. Western blot analysis of protein lysates from NSs grown for 16 hr in 4.5 or 1.0 g/L glucose revealed that low glucose was accompanied by elevated phosphorylation of CREB at Serine 133 (Ser133) (Figure 2A) and by increased transactivation of a cyclic AMP responsive element (CRE)-responsive luciferase reporter construct (Figure 2B), suggestive of elevated CREB transcriptional activity. Glucose regulation of CREB occurred upstream of the protein kinase A (PKA)-CREB cascade, because changes in CREB phosphorylation or activity closely mirrored differences in the intracellular content of cyclic AMP (cAMP) measured by ultrasensitive ELISA (Figure 2C). Moreover, the phosphodiesterase inhibitor Forskolin (Fsk) induced CREB(Ser133) phosphorylation, increased the expression of *Hes-1*, and increased the number of NSs in both high and low glucose. The PKA inhibitor, H-89, had the opposite effect and abolished the responses to glucose (Figures 2D and 2E). Overexpression of a non-phosphorylatable CREB mutant (mycCREB(S133A)) reduced Hes-1 mRNA and diminished NSC proliferative response to low glucose in a fashion that was completely rescued by co-transfection of Hes-1 (Figures 2F and 2H). Collectively, these findings strongly support roles for the cAMP-PKA cascade, for CREB phosphorylation on Ser133, and for Hes-1 expression in NSC regulation by glucose.

CREB Directly Regulates *Hes-1* Expression in NSCs

Prompted by the effect of the CREB(S133A) mutant on *Hes-1* expression, and to control for possible dominant-negative effects of this variant on other members of the CREB transcription factor family (Riccio et al., 2006), we purified NSCs from the hippocampus of mice homozygous for a "floxed" CREB allele ($CREB^{loxP/loxP}$) (Mantamadiotis et al., 2002) and induced permanent and highly specific CREB gene inactivation by adenoviral delivery of the *Cre* recombinase (Figure 3A). As previously reported (Dworkin et al., 2009), CREB deletion substantially reduced NS formation and DNA synthesis in standard, glucose-rich medium ($p < 0.001$, two-way ANOVA) (Figures 3B and 3C) compared to CREB-proficient (adenovirus [Ad] null-infected) cells. Most importantly, the increased proliferation of NSCs in response to low glucose was also lost in CREB-deficient cells (Figures 3B and 3C).

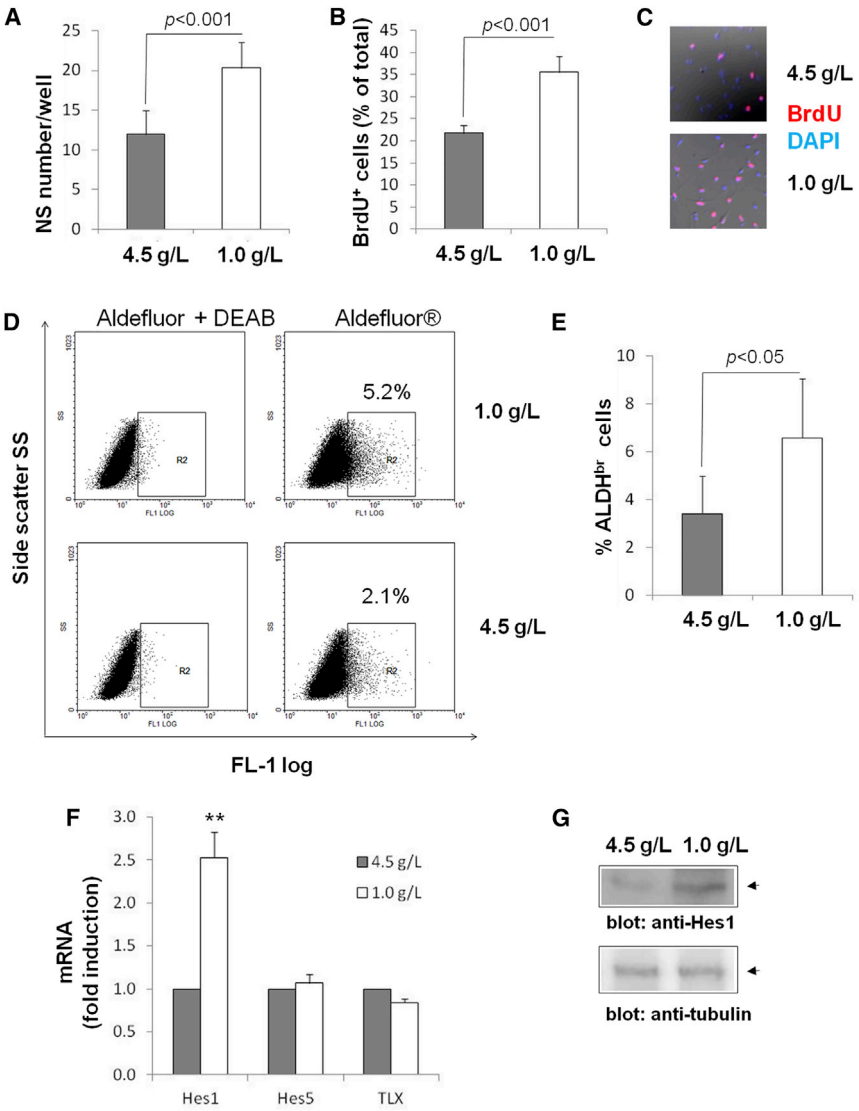

Figure 1. Ambient Glucose Affects NSC Self-Renewing Capacity In Vitro

(A) NSA: spheres (>50 μm diameter) formed over 7 days in low or high glucose from dissociated primary NSCs were counted under the microscope. Bar graph shows means ± SD of 10–12 wells from three independent experiments. Statistics by two-tailed t test.

(B) BrdU$^+$ cell counts from 15–20 independent microscopic fields. Statistics by two-tailed t test.

(C) Representative confocal scans of NSCs grown in 4.5 or 1.0 g/L glucose and immunostained for BrdU after 6 hr of incubation with the analog.

(D) Representative fluorescence-activated cell sorting (FACS) analysis of NSs dissociated after 5–7 days in 1.0 or 4.5 g/L glucose and labeled with the ALDH fluorescent substrate Aldefluor. Right plots: percentages of ALDH^{br} cells (region R2) in low and high glucose are indicated; the ALDH1-specific inhibitor diethylaminobenzaldehyde was used to confirm signal specificity and set the left boundary of R2 (left plots).

(E) Histogram displaying the mean ± SD of three independent FACS experiments. Numbers are raw percentages. Statistics by two-tailed paired t test.

(F) Real-time qRT-PCR analysis of *Hes-1*, *Hes-5*, and *TLX* mRNA expression in NSCs cultured in different glucose concentrations. Values are relative to expression in 4.5 g/L glucose and are mean ± SD of three independent experiments. Statistics by two-way ANOVA; $^{**}p < 0.01$ compared to 4.5 g/L.

(G) Western blot analysis confirming increased Hes-1 protein expression in NSCs grown in low glucose. Photograph is representative of several independent experiments.

See also Figure S1.

As seen earlier, *Hes-1* mRNA was upregulated by low glucose in CREB-proficient NSCs, while *Hes-1* expression was constitutively low and remarkably unresponsive to glucose in CREB-deficient NSCs (Figure 3D). This expression pattern closely mirrored that of established CREB target genes involved in mitochondrial function (*PGC-1 alpha*), metabolic homeostasis (*Sirt-1*) (Fusco et al., 2012b) and cell proliferation or differentiation (c-*fos*), raising the possibility that the expression of *Hes-1* may be directly regulated by CREB. As previously reported (Herzig et al., 2003), the promoter region of the murine *Hes-1* gene contains a conserved cAMP responsive half-site, located 231 base pairs upstream of the transcriptional start site (Zhang et al., 2005). Immunoprecipitation of cross-linked chromatin confirmed direct, glucose-responsive CREB binding to this DNA region in self-renewal growth conditions (Figure 3E). Increased promoter occupancy by CREB in low glucose required an intact Ser133 phosphorylation site, as revealed by the loss of inducible binding capacity of the CREB(S133A) mutant (Figures 3F and 3G). Control experiments performed under differentiative growth conditions revealed scarce CREB binding to the *Hes-1* promoter (Figure 3E).

Taken together, the preceding evidence identifies the phospho-CREB-dependent expression of *Hes-1* as a novel nutrient-sensing mechanism that links extracellular glucose with NSC renewal capacity in vitro.

The Deacetylase Sirt-1 Antagonizes CREB Action at the *Hes-1* Promoter and Is Necessary for NSC Inhibition by Glucose

The lysine deacetylase Sirt-1 cooperates with CREB in cellular nutrient sensing (Altarejos and Montminy, 2011; Fusco et al., 2012b) and has been previously shown to act as a repressor of *Hes-1* and *Hes-5* in differentiating neurons (Hisahara et al., 2008; Tiberi et al., 2012). This suggests that the Sirt-1 protein may participate in the CREB-dependent NSC response to glucose.

Chromatin immunoprecipitation (ChIP) studies showed that Sirt-1 binds to the CRE region upstream of *Hes-1*, with a pattern inverse to that of CREB; i.e., this interaction was stronger in high

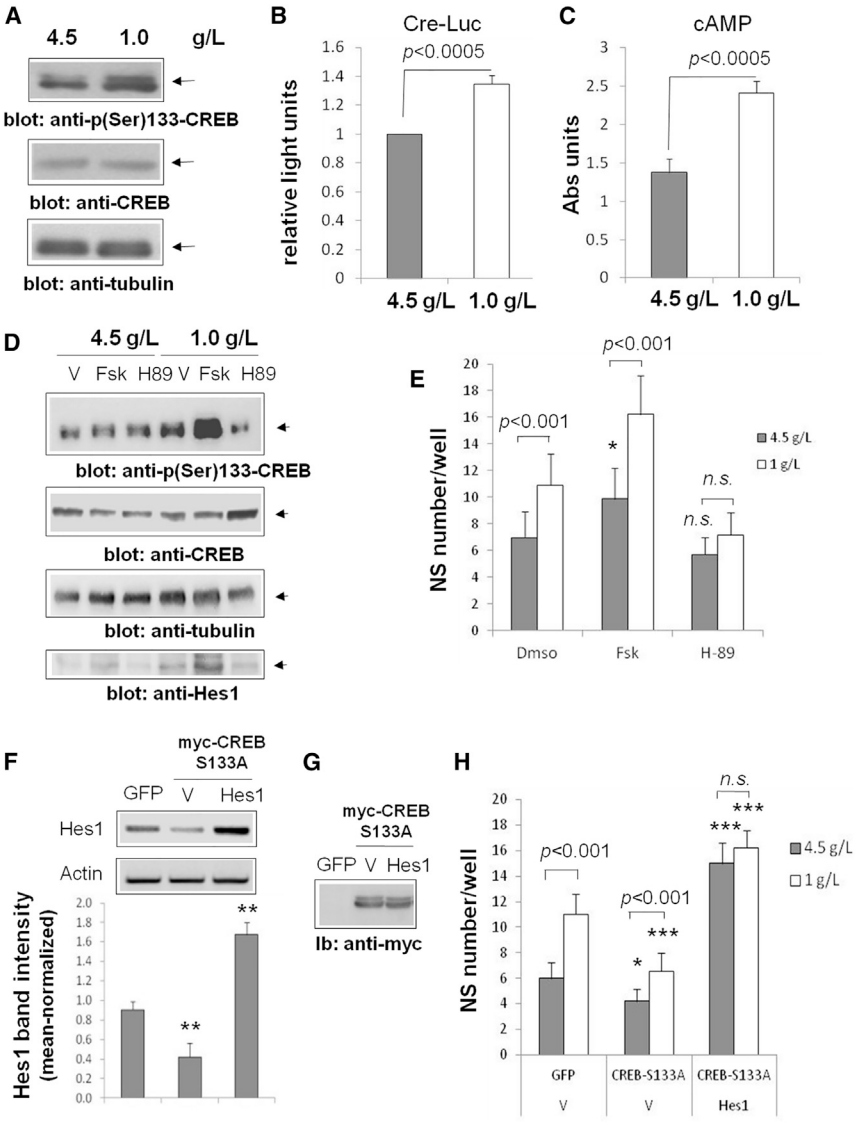

Figure 2. A cAMP-PKA-p^{Ser133}CREB-*Hes1* Cascade Mediates NSC Response to Glucose

(A) Anti-phospho(rylated) CREB(Ser133) phospho-specific immunoblotting showing reduced CREB phosphorylation in high glucose. Total CREB and tubulin (protein loading control) are also shown. Relevant bands are indicated by arrows. Representative of three independent experiments.

(B) The 6x-CRE-*Firefly luciferase* reporter assay showing globally reduced CREB activity after 16 hr of cell cultivation in high glucose. Values are normalized for transfection efficiency (*Renilla luciferase*) and are mean ± SD of three independent experiments in which the 4.5 g/L sample was set as a reference.

(C) Intracellular cAMP levels inversely correlate with extracellular glucose. Cells were processed as in (A), and cAMP was extracted and measured by ELISA with a commercial ultrasensitive kit. Values are in subtracted absorbance units, mean ± SD of two independent experiments each performed in duplicate.

(D) Effect of cAMP-PKA pharmacological modulation on glucose signaling to CREB. Cells were treated as (A) but in the presence of 10 μM Fsk (a functional PKA agonist), 1 μM H-89 (a selective PKA inhibitor), or DMSO as vehicle control (V). pCREB(Ser133), total CREB, and Hes-1 were monitored by immunoblotting. The blot shown is representative of at least two independent experiments.

(E) Effect of Fsk and H-89 on neural stem cell proliferation (NSA). Statistics by two-way ANOVA with Bonferroni post hoc analysis; *p < 0.05 compared to DMSO, 4.5 g/L; n = 18 from two independent experiments.

(F) Overexpression of the non-phosphorylatable mutant mycCREB(S133A) inhibits Hes-1 expression. After transfection with the indicated constructs, cells were grown for 16 hr in high glucose; Hes-1 mRNA was assessed by semi-qRT-PCR. Results of band densitometry from three independent experiments are reported in the histogram. Statistics by one way-ANOVA; **p < 0.01.

(G) Anti-myc immunoblotting confirming robust expression of the mycCREB(S133A) mutant in NSCs.

(H) NSA illustrating impaired proliferation and reduced glucose responsiveness of NSCs expressing CREB(S133A) and rescue by concomitant overexpression of Hes-1. Transfection efficiency was above 50% based on expression of GFP; V is an empty vector. Statistics as in (E); *p < 0.05 and ***p < 0.001 compared to mock-transfected (GFP+V) cells under the same glucose concentration.

glucose and in differentiation-inducing growth conditions and reduced in glucose-restricted cultures and in proliferation-inducing medium (Figure 4A, compare with Figure 3E). Acetylation of histone H3 at lysine 9 (Ac-H3K9), a substrate for Sirt-1 deacetylase activity (Vaquero et al., 2004), was more pronounced in low glucose (and in proliferating cells) (Figure 4A), consistent with active gene transcription in these conditions.

According with the idea that Sirt-1-dependent histone deacetylation around the CRE site contributes to Hes-1 transcriptional repression by high glucose, knockdown of Sirt-1 by a lentivirus-delivered short hairpin RNA increased baseline acetylation of the *Hes-1* promoter and disrupted sensitivity to glucose (Figure 4B). CREB binding to the same region remained glucose responsive in the absence of Sirt-1, suggesting that histone acetylation is not sufficient for CREB recruitment to the *Hes-1* CRE (Figure 4B, upper panel).

Hes-1 mRNA expression was increased in Sirt-1-deficient NSCs and was not or was poorly modulated by glucose (Figures 4C and 4D). Sirt-1 silencing also increased COX-IV expression, thus mimicking metabolic adaptation to low glucose (Figure S2), and most importantly, was accompanied by enhanced, glucose-insensitive NS formation in the NSA (Figure 4E). Taken together, the preceding observations identify Sirt-1 as part of the glucose-triggered molecular circuitry that attenuates NSC proliferation and self-renewal capacity. The Sirt-1 role appears to be antagonistic to, yet coordinated with, CREB action.

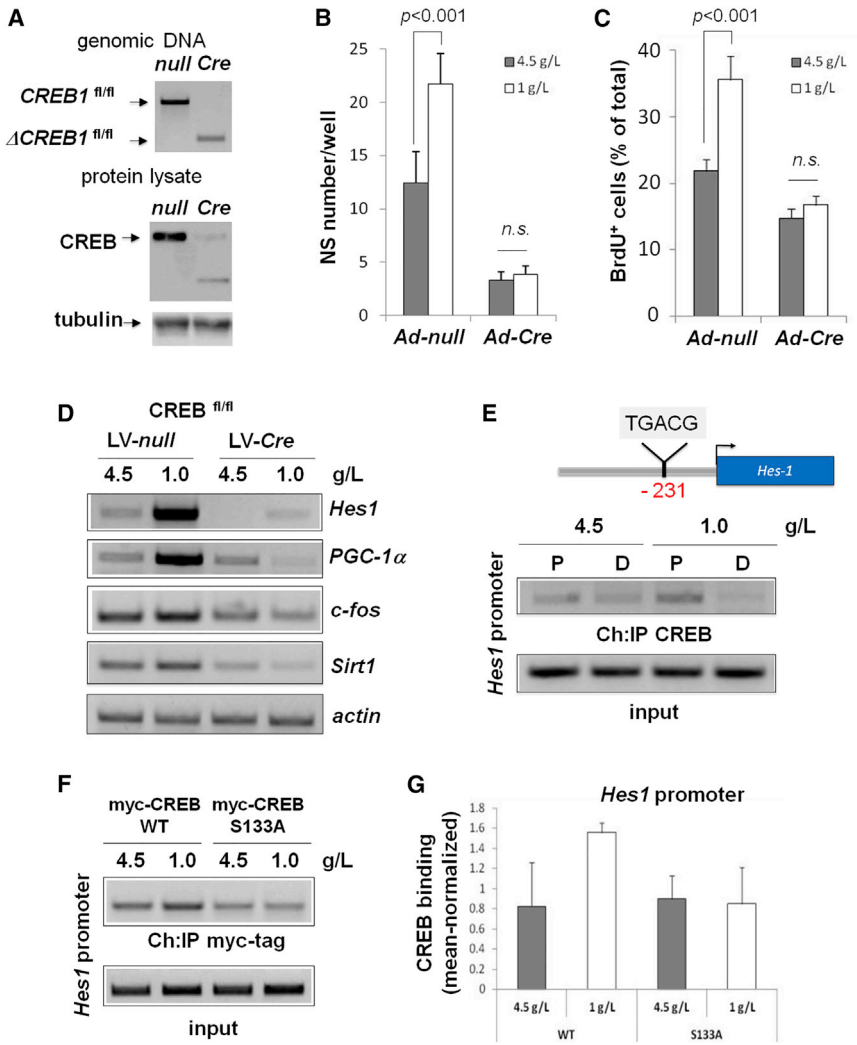

Figure 3. Direct Regulation of Hes-1 Expression by CREB in NSCs

(A–C) PCR (A, upper panel) and western blot analysis (A, lower panel) confirming successful deletion of CREB1 exon 10 in low-passage $CREB^{loxP/loxP}$ NSCs infected in vitro with the adenovirus encoding *Cre* recombinase (Ad-Cre) or the corresponding empty vector (Ad null) as control. (B and C) NSA and BrdU incorporation assays were performed as in Figure 1. (A and B) One week after cell infection with the indicated Ad vector. Values are means ± SD of 10–12 wells, and histograms are representative of at least two independent infection experiments. Statistics by two-way ANOVA; NS, not significant.

(D) Semi-qRT-PCR analysis of *Hes-1* expression, along with other CREB targets: *PGC-1 alpha*, c-*fos*, and *Sirt-1*. *Actin* was amplified as control for equal input mRNA. Photograph is representative of three independent experiments.

(E) ChIP analysis demonstrating glucose-dependent binding of CREB to the *Hes-1* promoter region flanking a semi-CRE element centered at position −231. Binding is more extensive in cells cultured under self-renewing (P, proliferative) compared to differentiative (D) growth conditions. Photograph is representative of two independent experiments.

(F) Anti-myc ChIP assay evaluating the interaction of myc-tagged WT and CREB(S133A) with the Hes-1 promoter in cells grown in 4.5 or 1.0 g/L glucose.

(G) Histogram plotting the mean ± SD of band quantitation from two independent experiments as in (F).

CREB Lysine 136 Participates in CREB-Sirt1 Interaction and Is Crucial for Glucose Sensing by CREB

Sirt-1 has been reported to directly downregulate CREB transcriptional activity by binding and deacetylating lysine 136 (K136), thereby reducing CREB interaction with the CREB binding protein (CBP) co-activator (Paz et al., 2014). CREB overall acetylation was markedly enhanced in NSCs exposed to the specific Sirt-1 inhibitors, sirtinol and nicotinamide, as revealed by anti-acetyl-lysine immunoblotting (Figure 5A). CREB acetylation was also induced by low glucose, consistent with increased CREB activity in this condition and in a fashion that was canceled by functional inactivation of Sirt-1 (Figure 5A). In keeping with previous reports (Qiang et al., 2011; Monteserin-Garcia et al., 2013), Sirt-1 depletion also led to increased CREB(Ser133) phosphorylation in nutrient-rich medium (Figures S3A and S3B), reinforcing the evidence that Sirt-1 directly modulates glucose signaling to CREB. Accordingly, reciprocal co-immunoprecipitation of Sirt-1 and CREB revealed that the two molecules form a complex and that their association is favored under low glucose conditions in which CREB acetylation is maximal (Figure 5B). This was still true when cell homogenates were normalized for their Sirt-1 content (right panels), which, as also seen in Figures 3D and 4C, was increased under glucose restriction (Figure 5B, top left panel).

To better characterize the molecular underpinnings of the CREB-Sirt1 interaction, both proteins were overexpressed in HEK293T cells with or without the CREB co-activator CBP to facilitate acetylation-dependent interactions (Figure 5C). These studies revealed that Sirt-1 binding to CREB was enhanced by CBP. The CBP-enhanced CREB-Sirt1 interaction requires CREB K136, a putative substrate for both CBP and Sirt-1 (Paz et al., 2014), because CBP failed to enhance Sirt-1 binding to CREB(K136A) (Figure 5C). CREB(K136A) bound more avidly than the wild-type (WT) CREB to CBP in 293T cells (Figure 5C) and, when expressed in NSCs, displayed glucose-independent hyperphosphorylation (Figure S3C). CREB(K136A) also drove hyperacetylation and overexpression of the *Hes-1* promoter (Figures 5D and 5E), as well as nutrient-insensitive cell over-proliferation (Figure 5F). These effects of the CREB(K136A) mutant are reminiscent of the effects of Sirt-1 depletion. However, CREB(K136A) was not recruited in low glucose to the *Hes-1* promoter (Figure 5D). Collectively, these findings suggest that both

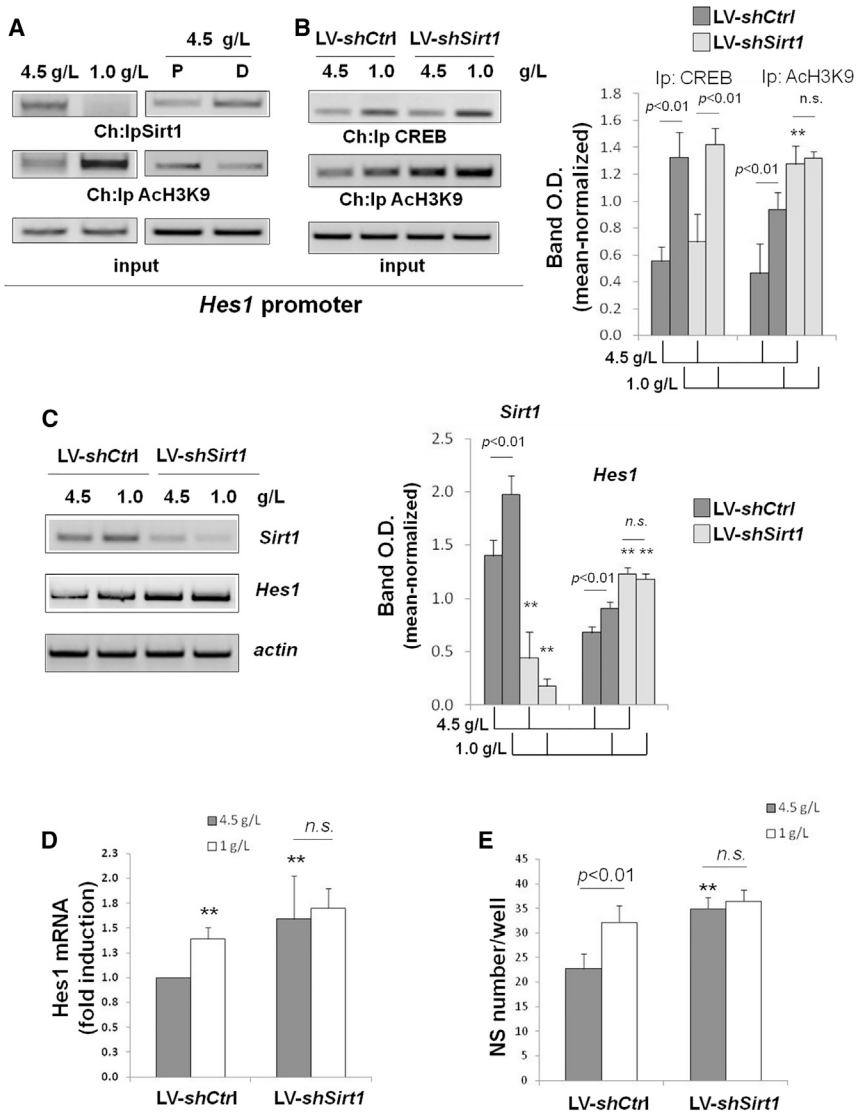

Figure 4. The Deacetylase Sirt-1 Antagonizes CREB Action at the *Hes-1* Promoter and Is Necessary for NSC Inhibition by Glucose

(A) ChIP studies illustrating Sirt-1 recruitment to the CRE region of the *Hes-1* promoter and deacetylation of H3K9 in this region. Culture conditions as in Figure 3E.

(B) ChIP studies illustrating the effect of Sirt-1 depletion on CREB binding and on accumulation of Ac-H3K9 at the Hes-1 CRE region. For each ChIP, the histogram displays mean ± SD of band intensity from three independent experiments. Dark gray columns are vectors encoding a short-hairpin RNA targeted against no known gene (shCtrl); light gray columns are vectors encoding a short-hairpin RNA targeted against Sirt-1 (shSirt-1). Statistics by 2×2 ANOVA; p values or NS (not significant) refer to glucose effects; asterisks (**p < 0.01) refer to shSirt-1 versus shCtrl.

(C) Semi-qRT-PCR analysis of *Sirt-1* and *Hes-1* mRNA expression in cells treated as in (B). Actin was amplified as the input control. Statistics as in (B).

(D) *Hes-1* mRNA expression was further quantified by real-time qRT-PCR analysis. Bars show means ± SD of six reactions (from two independent experiments); values are relative to the first bar (LV-shCtrl, 4.5 g/L). Statistics by two-way ANOVA.

(E) NSA illustrating the effect of Sirt-1 depletion in NSCs. Values are mean ± SD of 12 wells. Histogram is representative of two independent experiments. Statistics by two-way ANOVA; symbols as in (B) and (C).

See also Figure S2.

S133 and K136 of CREB play a role in glucose sensing and Hes-1 transcription, in keeping with the notion that these two residues act combinatorially in signal detection (Paz et al., 2014). These findings also suggest a role for Sirt-1, which antagonizes CREB activity and modulates its acetylation and phosphorylation. The effects of Sirt-1 on CREB appear to be mediated by physical interaction with CREB dependent on K136 and CBP.

The CREB-Sirt1-Hes1 Circuitry Is Activated in Mouse Hippocampus by CR

Because CR is accompanied in mice by lower blood glucose levels, Sirt-1 induction in the brain, and preserved neurogenesis during aging (Lee et al., 2000; Mattson, 2000; Cohen et al., 2004), we speculated that the glucose sensitive CREB-Sirt1-Hes1 circuitry could be relevant in this physiological setting.

Mice subjected to a 20%–30% CR for a period of 6 weeks (Fusco et al., 2012b) displayed markedly reduced plasma glucose concentrations compared to animals fed ad libitum (AL) (Figure S4). Five days before sacrifice, both groups of animals were injected with BrdU (100 μg/kg) to label the proliferating NSC pool. Double immunostaining of hippocampal sections for BrdU and Nestin (Nes, a NSC marker) revealed that CR increased the number of proliferating NSCs ($BrdU^+/Nes^+$) in the subgranular zone of the DG (Figures 6A and 6B).

Consistent with changes observed in low-glucose NSCs in vitro, the RT-PCR of total hippocampal RNA from CR mice showed a significant increase in *Hes-1* mRNA abundance ($p < 0.05$) (Figures 6C and 6D). A similar analysis conducted on total brain homogenates from calorie-restricted Sirt-1 knockout (KO) mice and their control littermates revealed that, just like in NSCs, Hes-1 expression was abnormally elevated and refractory to further increase with CR (Figure 6D). According with our in vitro findings, CR substantially increased CREB occupancy at the *Hes-1* promoter ($p < 0.05$) in the hippocampus. Sirt-1 bound to the same CRE site was reduced by CR, and this change was accompanied by the accumulation of the Ac-H3K9, a marker of active transcription ($p < 0.05$) (Figures 6E and 6F).

Thus, despite the profound difference of complexity between the in vitro and the in vivo models, the preceding findings confirm that the nutrient-sensitive transcriptional circuitry involving

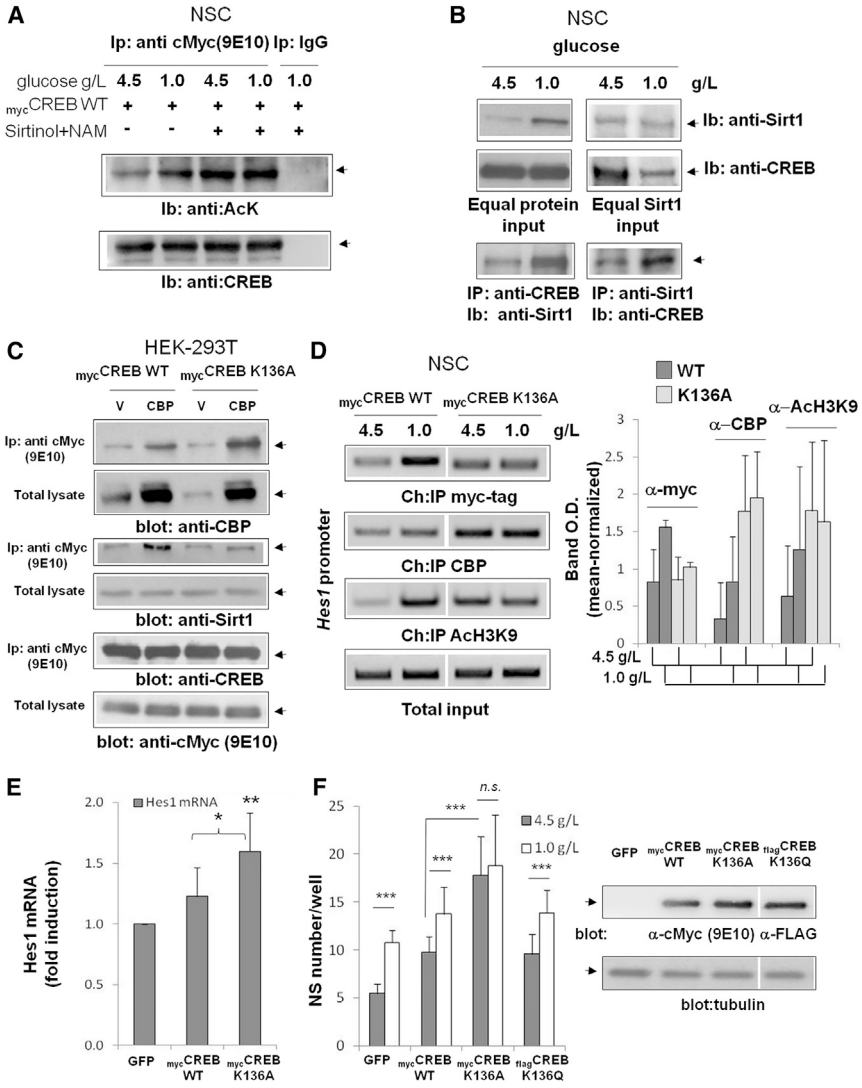

Figure 5. CREB K136 Participates in CREB-Sirt1 Interaction and in Glucose Sensing by CREB

(A) Immunoprecipitation and western blot analysis showing enhanced acetylation of CREB in response to low glucose or to the Sirt-1 inhibitors, sirtinol and nicotinamide. To facilitate biochemical analysis of post-translational modifications, a myc-tagged recombinant CREB was overexpressed in NSCs. Glucose concentration and the presence or absence of inhibitors are indicated. Relevant bands are marked by arrows. Photograph is representative of two independent experiments.

(B) Immunoprecipitation and western blot analysis revealing reciprocal co-precipitation of Sirt-1 and CREB in NSCs and increased interaction of these proteins in low glucose. Sirt-1 immunoprecipitation was performed after lysate normalization for Sirt-1 content (compare upper left and upper right panels). This leads to overcompensation for total CREB. Immunostaining of total lysates is also depicted.

(C) Western blot analysis of CREB-Sirt1 co-immunoprecipitation in HEK293T cells. Transfected plasmids and antibodies used for immunoprecipitation and immunoblotting are indicated. Immunoblotting of input protein lysates are shown as a control. The CREB(K136A) mutant displays lower binding to Sirt-1 and higher binding to CBP. All experiments were performed in 4.5 g/L glucose. Photograph is representative of two independent experiments.

(D) ChIP analysis showing glucose-insensitive binding of CREB(K136A) to the Hes-1 CRE region, similar glucose-insensitive binding of CBP, and constitutive promoter acetylation in cells expressing CREB(K136A). Histogram bars are mean ± SD from two independent experiments. Dark gray is WT CREB; light gray is CREB(K136A).

(E) The qPCR analysis of Hes-1 expression in NSCs transfected with GFP, WT CREB, or CREB (K136A). Statistics by one-way ANOVA. *$p < 0.05$ between WT and K136A; **$p < 0.01$ compared to GFP.

(F) NSA illustrating the effect of different CREB mutants on NSC proliferation and self-renewal. Statistics by two-way ANOVA. Asterisks (***$p < 0.001$) denote glucose effects; p value for K136A versus WT is also indicated. Data are from two independent experiments with n = 12.

See also Figure S3.

CREB, Sirt-1, and Hes-1 could have a role in the connection between reduced nutrient availability and enhanced neurogenesis.

DISCUSSION

We have described a molecular circuitry that regulates NSC proliferation and self-renewal in response to changes in glucose concentration. Although the main components of this nutrient-sensing switch, CREB and Sirt-1, have well recognized roles at the crossroads of nutrient sensing, energy metabolism, and cell or tissue aging (Altarejos and Montminy, 2011; Fusco et al., 2012a) and have already been implicated in the regulation of NSC renewal, survival, and differentiation (Dworkin et al., 2009; Hisahara et al., 2008; Prozorovski et al., 2008; Saharan et al., 2013; Ma et al., 2014), we identified a key role for the glucose-sensing CREB-Sirt1-*Hes1* network in the regulation of NSC behavior.

Most current protocols recommend NSC cultivation in the presence of supra-physiological concentrations of glucose, close to those employed in studies of cell hyperglycemic damage (Du et al., 2000). We showed that NSCs display better self-renewal capacity in physiological glucose levels, which suggested that glucose excess may limit NSC function and lifespan in the context of hyperglycemic conditions such as diabetes. While our in vitro studies on NSCs involved modulating only glucose concentrations, it is remarkable that the *CREB-Sirt1-Hes1* axis was found in vivo in mice under CR, which strongly argues in support of its physiological relevance despite the much higher complexity of whole animal nutrition. We identified the cAMP-PKA pathway as the cascade that signals glucose

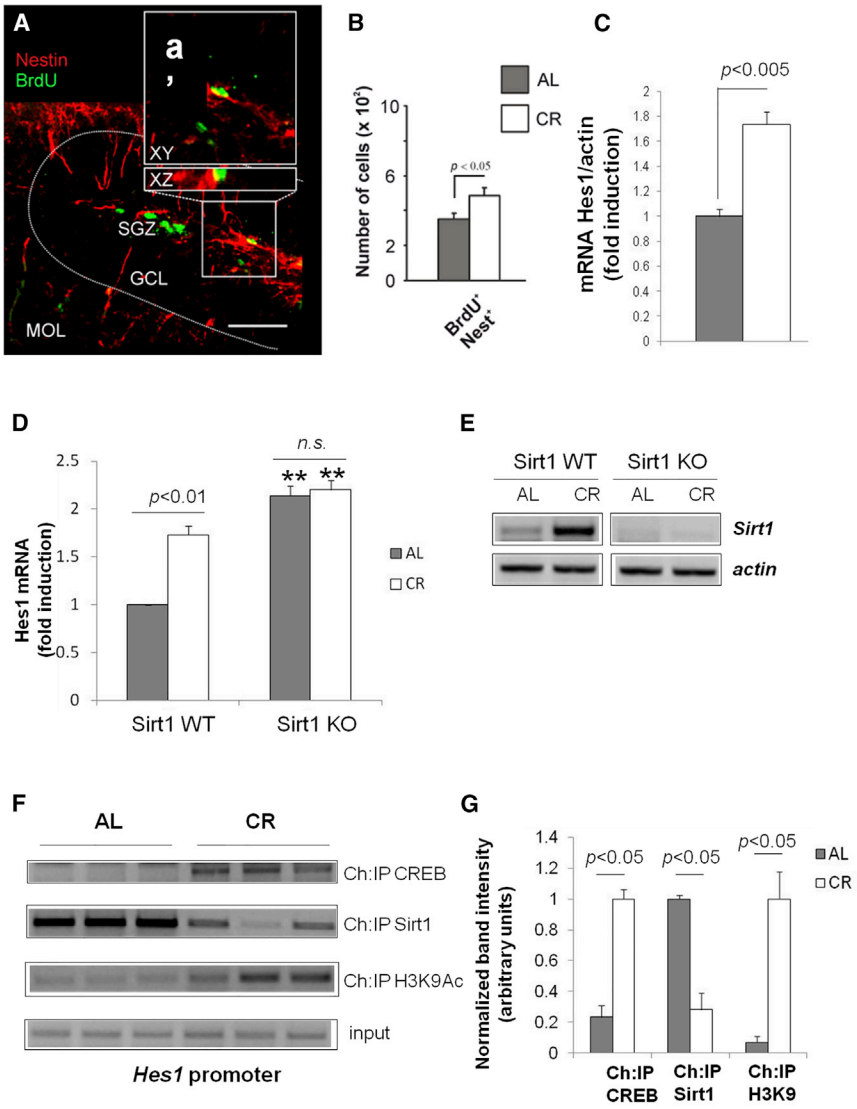

Figure 6. The CREB-Sirt1-Hes1 Circuitry Is Activated in Mouse Hippocampus by CR

(A) Representative confocal image of coronal brain section double labeled for BrdU (green) and Nes (red). The dotted line indicates the edge of the DG of the hippocampus. MOL, molecular layer; GCL, granule cell layer; SGZ, subgranular zone. Scale bar, 75 μm. (A′) High-magnification xy image of the box-delimited regions of (A). The xz cross section from the z stack acquisitions shows co-localization of BrdU and Nes in a representative NSC of the SGZ.

(B) Bar graph showing the number (mean ± SEM) of proliferating NSCs ($BrdU^+/Nes^+$) in the SGZ of AL (gray bar) and CR mice (white bar). Statistics by Mann-Whitney test.

(C) CR induces *Hes-1* mRNA expression in the hippocampus, as revealed by semi-qRT-PCR analysis of *Hes-1* mRNA expression in whole hippocampi of AL and CR mice. Histogram shows the mean ± SEM of band densitometric values from three independent animals. Statistics by Mann-Whitney test.

(D and E) Brain Sirt-1 is induced by CR and downregulates *Hes-1* expression in vivo. (D) Real-time PCR analysis of whole brain mRNA from WT and Sirt-1 KO mice under AL or CR feeding regimens. Hes-1 expression is constitutively elevated in the brain of Sirt-1 KO mice and is not modulated by calorie intake. Bars are means ± SEM of four animals per genotype per feeding regimen. Statistics by 2×2 ANOVA; p values or NS (not significant) refer to diet effect in each mouse strain; asterisks (**$p < 0.01$) refer to comparisons between Sirt-1 genotypes. (E) Representative RT-PCR analysis confirming strong downregulation of brain Sirt-1 mRNA in Sirt-1 (exons 5 and 6) KO mice. Note Sirt-1 upregulation by CR in WT mice.

(F and G) ChIP studies revealing coordinated CREB and Sirt-1 occupancy of the *Hes-1* promoter in the hippocampi of mice under different dietary regimens (AL or CR). Histogram reports band quantitation from (F) and statistics by Mann-Whitney test. Values are mean ± SEM of three mice. See also Figure S4.

availability to CREB (Figures 2C and 2D) and showed that CREB(Ser133) phosphorylation was crucial for glucose-regulated *Hes-1* promoter occupancy and transactivation (Figures 2F and 3F). The glucose-regulated biochemical events upstream of cAMP remain elusive, although cAMP levels signal extracellular glucose in yeast (Kim et al., 2013). Modulation of the Notch pathway can also affect Hes-1 expression (Kageyama and Ohtsuka, 1999) by glucose-mediated protein modifications (Brückner et al., 2000; Guo et al., 2013), an aspect to be further investigated in our experimental model.

Our results suggest that Sirt-1 association with, and deacetylation of, the *Hes-1* chromatin surrounding a CRE regulatory region participates in signaling the "off" status of the transcriptional switch (Figure 7). Nutrient-dependent dissociation of Sirt-1 from this region, possibly because of the inducible binding of CREB, allows for promoter acetylation and *Hes-1* transcription, while indiscriminate depletion of Sirt-1 (as in gene knockdown experiments depicted in Figures 4C–4E) leads to glucose-insensitive promoter activation and to NSC expansion. This latter finding, mirrored by *Hes-1* mRNA analysis in the brain of Sirt-1 KO mice (Figure 6), confirms recent reports of increased proliferation (and rapid exhaustion) of NSCs in Sirt-1-deficient adult brain cells in vitro and in vivo (Rafalski et al., 2013; Ma et al., 2014).

ChIP studies show that CREB is dynamically recruited to the *Hes-1* CRE element under low glucose and that this response is preserved even when Sirt-1 is depleted (Figure 4B). Inducible CREB binding is critically dependent on both Ser133 (Figure 3F) and K136 (Figure 5D), two residues recently shown to act combinatorially, when phosphorylated and acetylated, respectively, to integrate coincident signals (Paz et al., 2014). Increased affinity of doubly modified (phosphorylated and acetylated) CREB for the co-activator CBP histone acetyltransferase may play a role in glucose-enhanced CREB binding to the *Hes-1* promoter and

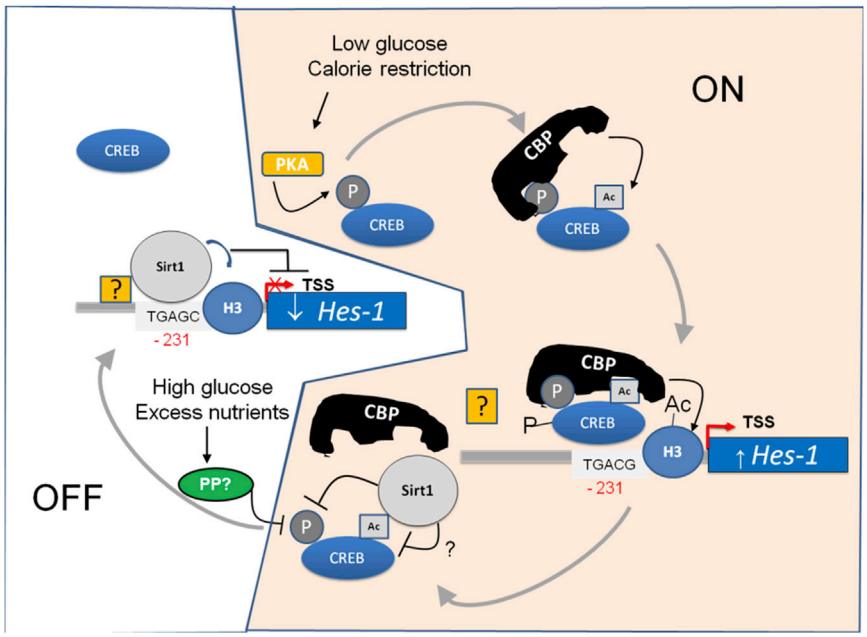

Figure 7. Model of CREB-Sirt1-Hes1 Transcriptional Circuitry Modulating NSC Proliferation and Self-Renewal in Response to Glucose

Model summarizing the main findings of the study. In high glucose ("off" state, white background) Sirt-1 deacetylases and represses Hes-1 chromatin; in low glucose ("on" state, ivory background), doubly modified CREB (P-Ser133; Ac-K136) displaces Sirt-1 at the Hes-1 CRE region, and activates transcription. In low glucose, Sirt-1 and CREB associate in the nucleoplasm, where CREB acetylation and phosphorylation are downregulated. In high glucose, PKA activity is reduced, CREB is dephosphorylated and deacetylated, and the circuitry returns to the "off" state.

facilitates CRE occupancy at the expense of Sirt-1 (Figures 3E, 4A, and 7). In keeping with this view, CREB acetylation is also increased, coincident with phosphorylation, in low ambient glucose (Figure 5A).

Evidence of physical association between CREB and Sirt-1 adds further complexity to the picture. Based on mechanistic studies in HEK293T cells, binding between these two proteins is increased by CBP, possibly by CBP-dependent CREB acetylation at lysine 136 (Ac-K136). This is in agreement with the finding that CREB-Sirt1 binding is enhanced in the "on" state (low glucose) (Figure 5B). However, Sirt-1 and CREB were not detected in a complex on *Hes-1* chromatin in ChIP experiments (Figure 7) perhaps because Sirt-1 targets the pool of doubly phosphorylated and acetylated CREB that transiently dissociated from CBP and from chromatin. We believe that Sirt-1 is a direct inhibitor of CREB because CREB acetylation was markedly enhanced by Sirt-1 inhibitors (Figure 5A) and because downregulation of Sirt-1 or substitution of CREB K136 with Alanine, a mutation that reduces CREB binding capacity to Sirt-1 (Figure 5B), promotes glucose-resistant CREB phosphorylation in NSCs (Figures S3B and S3C). Mechanistically, Sirt-1 may, in addition to binding and deacetylating K136, enhance CREB dephosphorylation (Monteserin-Garcia et al., 2013). Accordingly, overexpression of the CREB(K136A) mutant phenocopies in NSCs the consequences of Sirt-1 depletion, including high expression of *Hes-1* (Figure 5F) and deregulated glucose-insensitive proliferative capacity (Figure 5F). Instead, overexpression of the CREB(K136Q) mutant, which mimics Ac-K136 (Qiang et al., 2011), increased proliferation to the same extent as CREB and did not disrupt NSC responsiveness to glucose (Figure 5F). While CREB(Ser133) phosphorylation seems important for the extent of Hes-1 transactivation in NSCs, how Hes-1 expression is finely tuned by modifications of CREB at K136 and to what extent those involve Sirt-1 remains to be clarified. Results of our ChIP studies also suggest that Sirt-1 interaction with the CRE region in high glucose is largely CREB independent and may thus involve different DNA binding complexes (Figure 7, orange box), such as the transcriptional repressor Bcl-6 (Tiberi et al., 2012).

In conclusion, although further molecular characterization and validation in vivo would be worthwhile, the nutrient-sensitive CREB-Sirt1-Hes1 circuitry described here extends our knowledge of nutrient sensing by NSC and, by extension, of the metabolic regulation in adult neurogenesis. This network could coordinate neurogenic activity with body metabolic status and limit indiscriminate exhaustion of the stem and progenitor pool. The response of this network to metabolic disorders may mediate some of the detrimental consequences of these metabolic disorders on brain functions and shed light on the emerging association between diabetes and Alzheimer's disease (Haan, 2006).

EXPERIMENTAL PROCEDURES

Mice

All experimental procedures were performed according to international standards of animal care and had been previously approved by the Institutional Ethical Committee. For CR studies, the amount of food consumed AL was determined weekly, and CR mice were fed daily 80% of that value for the first week and 70% for the following 5 weeks.

Cell Culture

Postnatal hippocampal NSC cultures were isolated from newborn C57BL/6 mice according to a previously published protocol (Leone et al., 2014; Podda et al., 2014).

In Vitro Analyses of NSC Self-Renewal and Proliferation

NSAs and BrdU incorporation were used to assess the effects of low and high glucose concentrations on secondary NS formation (self-renewal) and NSC proliferation, respectively.

Neurosphere Assay

In brief, a single-cell suspension from dissociated NSs was plated in a 96-well plate at a density of 2,000 cells/well in proliferative medium containing low (1.0 g/L) or high (4.5 g/L) glucose concentrations. Fsk and H-89 were added fresh every 2 days. After 7 days of culture, the number and the size of secondary NSs ($\geq$50 μm diameter) were analyzed in both groups using an inverted microscope equipped with an eyepiece graticule and Zeiss Axiovision digital

image processing software (Renault et al., 2009). The operator was blind to the culture conditions.

BrdU Incorporation Analysis

Undifferentiated NSCs obtained by NS dissociation were plated onto round coverslips and left to proliferate for 24 hr. After this period, BrdU (2.5 μM) was added to the NSC culture medium, and the cultures were incubated in either low or high glucose conditions for 6 hr before fixation. Cells incorporating BrdU were identified by immunocytochemistry, as previously described (Leone et al., 2014).

ChIP Studies

ChIP assays were performed as previously described (Leone et al., 2014). For NSCs, 1.5×10^6 cells grown in proliferation and differentiation medium were used per ChIP. Five coronal brain sections containing hippocampi were used for each animal (n = 6 CR mice; n = 6 AL mice). Hippocampal areas were isolated under the optical microscope and minced through a 10 ml syringe with decreasing needle size (18G–22G). Cell or tissue lysates were resuspended in 200 μl lysis buffer containing SDS (1%), Tris-HCl (50 mM, pH 8.1), and EDTA (10 mM) and were sonicated on ice with six 10 s pulses with a 20 s interpulse interval. Sample debris was removed by centrifugation, and supernatants were subjected to immunoprecipitation with specific antisera. DNA fragments were purified by using the PCR DNA fragment purification kit (Geneaid Biotech). PCR conditions and cycle numbers were determined empirically for the different templates and primer pairs.

Analysis of Adult Neurogenesis In Vivo

All animals received for 5 consecutive days an intraperitoneal injection of BrdU (Sigma; 100 mg/kg dissolved in 0.9% NaCl solution). On the fifth day, mice were deeply anesthetized with a cocktail of ketamine (100 mg/ml) and medetomidine (1 mg/ml; ratio: 5:3) and were transcardially perfused with PBS solution, followed by 4% paraformaldehyde fixative solution. Coronal sections (40 μm thick) were then cut with a vibratome (VT1000S, Leica Microsystems), immunoprocessed, and counted under the 63× objective of a confocal laser scanning microscope (TCS-SP2, Leica Microsystems) as previously described (Leone et al., 2014).

Statistics

Statistics was performed with Sigma Plot 12.0 (Systat Software). Values were expressed as either mean ± SD (experiments in vitro) or mean ± SEM (experiments with mice). Statistical significance of mean differences was determined by (unpaired or paired) two-tailed t test or by Mann-Whitney test (for small datasets). Two-way ANOVA (with Tukey Honest Significant Difference post hoc analysis) was used for multiple comparisons. Differences were considered significant for $p < 0.05$.

SUPPLEMENTAL INFORMATION

Supplemental Information includes Supplemental Experimental Procedures and four figures and can be found with this article online at http://dx.doi.org/10.1016/j.celrep.2015.12.092.

AUTHOR CONTRIBUTIONS

G.P. and C.G. conceived the study and co-supervised the work; S.F. and L.L. designed and performed most experiments and analyzed data with supervisors; S.A.B. performed studies of neurogenesis in vivo; G.T. prepared viral constructs; G.M. measured ROS; R.P. performed immunocytochemical experiments and confocal microscopy analysis; D.S. and M.S. contributed to the western blotting experiments; M.M. provided samples from Sirt-1 KO mice and analyzed data; G.P. wrote the paper; and all authors commented on the manuscript and approved its final version.

ACKNOWLEDGMENTS

This work was supported by intramural grants from Catholic University (Linea D.3.2-2013 and Linea D.1 to C.G. and G.P.), by the Italian Association for Cancer Research (AIRC, grant IG 2014 Id.15381 to G.P.), by the Italian Ministry of Foreign Affairs (PGR-2015 to G.P.), by the Italian Ministry of University and Research (SIR 2014 RBSI14ZV59 to S.F.), by the Italian Ministry of Health (GR-2011-02352187 to S.F. and R.P.), and by Fondazione Roma (Call for Non Communicable Diseases 2014 to G.P.). The authors wish to acknowledge Dr. Antonella Riccio (London, UK) for reagents and helpful comments.

Received: August 11, 2015
Revised: August 21, 2015
Accepted: December 20, 2015
Published: January 21, 2016

REFERENCES

Aguirre, A., Rubio, M.E., and Gallo, V. (2010). Notch and EGFR pathway interaction regulates neural stem cell number and self-renewal. Nature *467*, 323–327.

Altarejos, J.Y., and Montminy, M. (2011). CREB and the CRTC co-activators: sensors for hormonal and metabolic signals. Nat. Rev. Mol. Cell Biol. *12*, 141–151.

Bondolfi, L., Ermini, F., Long, J.M., Ingram, D.K., and Jucker, M. (2004). Impact of age and caloric restriction on neurogenesis in the dentate gyrus of C57BL/6 mice. Neurobiol. Aging *25*, 333–340.

Brückner, K., Perez, L., Clausen, H., and Cohen, S. (2000). Glycosyltransferase activity of Fringe modulates Notch-Delta interactions. Nature *406*, 411–415.

Cohen, H.Y., Miller, C., Bitterman, K.J., Wall, N.R., Hekking, B., Kessler, B., Howitz, K.T., Gorospe, M., de Cabo, R., and Sinclair, D.A. (2004). Calorie restriction promotes mammalian cell survival by inducing the SIRT1 deacetylase. Science *305*, 390–392.

Corti, S., Locatelli, F., Papadimitriou, D., Donadoni, C., Salani, S., Del Bo, R., Strazzer, S., Bresolin, N., and Comi, G.P. (2006). Identification of a primitive brain-derived neural stem cell population based on aldehyde dehydrogenase activity. Stem Cells *24*, 975–985.

Cukierman, T., Gerstein, H.C., and Williamson, J.D. (2005). Cognitive decline and dementia in diabetes—systematic overview of prospective observational studies. Diabetologia *48*, 2460–2469.

Deleyrolle, L.P., Ericksson, G., Morrison, B.J., Lopez, J.A., Burrage, K., Burrage, P., Vescovi, A., Rietze, R.L., and Reynolds, B.A. (2011). Determination of somatic and cancer stem cell self-renewing symmetric division rate using sphere assays. PLoS ONE *6*, e15844.

Du, X.L., Edelstein, D., Rossetti, L., Fantus, I.G., Goldberg, H., Ziyadeh, F., Wu, J., and Brownlee, M. (2000). Hyperglycemia-induced mitochondrial superoxide overproduction activates the hexosamine pathway and induces plasminogen activator inhibitor-1 expression by increasing Sp1 glycosylation. Proc. Natl. Acad. Sci. USA *97*, 12222–12226.

Dworkin, S., Malaterre, J., Hollande, F., Darcy, P.K., Ramsay, R.G., and Mantamadiotis, T. (2009). cAMP response element binding protein is required for mouse neural progenitor cell survival and expansion. Stem Cells *27*, 1347–1357.

Fusco, S., Maulucci, G., and Pani, G. (2012a). Sirt1: def-eating senescence? Cell Cycle *11*, 4135–4146.

Fusco, S., Ripoli, C., Podda, M.V., Ranieri, S.C., Leone, L., Toietta, G., McBurney, M.W., Schütz, G., Riccio, A., Grassi, C., et al. (2012b). A role for neuronal cAMP responsive-element binding (CREB)-1 in brain responses to calorie restriction. Proc. Natl. Acad. Sci. USA *109*, 621–626.

Gage, F.H. (2000). Mammalian neural stem cells. Science *287*, 1433–1438.

Guo, Y., Wang, P., Sun, H., Cai, R., Xia, W., and Wang, S. (2013). Advanced glycation end product-induced astrocytic differentiation of cultured neurospheres through inhibition of Notch-Hes1 pathway-mediated neurogenesis. Int. J. Mol. Sci. *15*, 159–170.

Gur, T.L., Conti, A.C., Holden, J., Bechtholt, A.J., Hill, T.E., Lucki, I., Malberg, J.E., and Blendy, J.A. (2007). cAMP response element-binding protein deficiency allows for increased neurogenesis and a rapid onset of antidepressant response. J. Neurosci. *27*, 7860–7868.

Haan, M.N. (2006). Therapy insight: type 2 diabetes mellitus and the risk of late-onset Alzheimer's disease. Nat. Clin. Pract. Neurol. *2*, 159–166.

Herzig, S., Hedrick, S., Morantte, I., Koo, S.H., Galimi, F., and Montminy, M. (2003). CREB controls hepatic lipid metabolism through nuclear hormone receptor PPAR-gamma. Nature *426*, 190–193.

Hisahara, S., Chiba, S., Matsumoto, H., Tanno, M., Yagi, H., Shimohama, S., Sato, M., and Horio, Y. (2008). Histone deacetylase SIRT1 modulates neuronal differentiation by its nuclear translocation. Proc. Natl. Acad. Sci. USA *105*, 15599–15604.

Ito, K., Hirao, A., Arai, F., Matsuoka, S., Takubo, K., Hamaguchi, I., Nomiyama, K., Hosokawa, K., Sakurada, K., Nakagata, N., et al. (2004). Regulation of oxidative stress by ATM is required for self-renewal of haematopoietic stem cells. Nature *431*, 997–1002.

Jang, Y.Y., and Sharkis, S.J. (2007). A low level of reactive oxygen species selects for primitive hematopoietic stem cells that may reside in the low-oxygenic niche. Blood *110*, 3056–3063.

Kageyama, R., and Ohtsuka, T. (1999). The Notch-Hes pathway in mammalian neural development. Cell Res. *9*, 179–188.

Kim, J.H., Roy, A., Jouandot, D., 2nd, and Cho, K.H. (2013). The glucose signaling network in yeast. Biochim. Biophys. Acta *1830*, 5204–5210.

Kippin, T.E., Martens, D.J., and van der Kooy, D. (2005). p21 loss compromises the relative quiescence of forebrain stem cell proliferation leading to exhaustion of their proliferation capacity. Genes Dev. *19*, 756–767.

Lang, B.T., Yan, Y., Dempsey, R.J., and Vemuganti, R. (2009). Impaired neurogenesis in adult type-2 diabetic rats. Brain Res. *1258*, 25–33.

Lee, J., Duan, W., Long, J.M., Ingram, D.K., and Mattson, M.P. (2000). Dietary restriction increases the number of newly generated neural cells, and induces BDNF expression, in the dentate gyrus of rats. J. Mol. Neurosci. *15*, 99–108.

Leone, L., Fusco, S., Mastrodonato, A., Piacentini, R., Barbati, S.A., Zaffina, S., Pani, G., Podda, M.V., and Grassi, C. (2014). Epigenetic modulation of adult hippocampal neurogenesis by extremely low-frequency electromagnetic fields. Mol. Neurobiol. *49*, 1472–1486.

Ma, C.Y., Yao, M.J., Zhai, Q.W., Jiao, J.W., Yuan, X.B., and Poo, M.M. (2014). SIRT1 suppresses self-renewal of adult hippocampal neural stem cells. Development *141*, 4697–4709.

Magri, L., Cambiaghi, M., Cominelli, M., Alfaro-Cervello, C., Cursi, M., Pala, M., Bulfone, A., Garcia-Verdugo, J.M., Leocani, L., Minicucci, F., et al. (2011). Sustained activation of mTOR pathway in embryonic neural stem cells leads to development of tuberous sclerosis complex-associated lesions. Cell Stem Cell *9*, 447–462.

Mantamadiotis, T., Lemberger, T., Bleckmann, S.C., Kern, H., Kretz, O., Martin Villalba, A., Tronche, F., Kellendonk, C., Gau, D., Kapfhammer, J., et al. (2002). Disruption of CREB function in brain leads to neurodegeneration. Nat. Genet. *31*, 47–54.

Mattson, M.P. (2000). Neuroprotective signaling and the aging brain: take away my food and let me run. Brain Res. *886*, 47–53.

Messier, C. (2005). Impact of impaired glucose tolerance and type 2 diabetes on cognitive aging. Neurobiol. Aging *26* (*Suppl 1*), 26–30.

Monteserin-Garcia, J., Al-Massadi, O., Seoane, L.M., Alvarez, C.V., Shan, B., Stalla, J., Paez-Pereda, M., Casanueva, F.F., Stalla, G.K., and Theodoropoulou, M. (2013). Sirt1 inhibits the transcription factor CREB to regulate pituitary growth hormone synthesis. FASEB J. *27*, 1561–1571.

Nakagawa, S., Kim, J.E., Lee, R., Malberg, J.E., Chen, J., Steffen, C., Zhang, Y.J., Nestler, E.J., and Duman, R.S. (2002). Regulation of neurogenesis in adult mouse hippocampus by cAMP and the cAMP response element-binding protein. J. Neurosci. *22*, 3673–3682.

Ohtsuka, T., Sakamoto, M., Guillemot, F., and Kageyama, R. (2001). Roles of the basic helix-loop-helix genes Hes1 and Hes5 in expansion of neural stem cells of the developing brain. J. Biol. Chem. *276*, 30467–30474.

Panieri, E., Toietta, G., Mele, M., Labate, V., Ranieri, S.C., Fusco, S., Tesori, V., Antonini, A., Maulucci, G., De Spirito, M., et al. (2010). Nutrient withdrawal rescues growth factor-deprived cells from mTOR-dependent damage. Aging (Albany, N.Y.) *2*, 487–503.

Park, H.R., and Lee, J. (2011). Neurogenic contributions made by dietary regulation to hippocampal neurogenesis. Ann. N Y Acad. Sci. *1229*, 23–28.

Paz, J.C., Park, S., Phillips, N., Matsumura, S., Tsai, W.W., Kasper, L., Brindle, P.K., Zhang, G., Zhou, M.M., Wright, P.E., and Montminy, M. (2014). Combinatorial regulation of a signal-dependent activator by phosphorylation and acetylation. Proc. Natl. Acad. Sci. USA *111*, 17116–17121.

Podda, M.V., Leone, L., Barbati, S.A., Mastrodonato, A., Li Puma, D.D., Piacentini, R., and Grassi, C. (2014). Extremely low-frequency electromagnetic fields enhance the survival of newborn neurons in the mouse hippocampus. Eur. J. Neurosci. *39*, 893–903.

Prozorovski, T., Schulze-Topphoff, U., Glumm, R., Baumgart, J., Schröter, F., Ninnemann, O., Siegert, E., Bendix, I., Brüstle, O., Nitsch, R., et al. (2008). Sirt1 contributes critically to the redox-dependent fate of neural progenitors. Nat. Cell Biol. *10*, 385–394.

Qiang, L., Lin, H.V., Kim-Muller, J.Y., Welch, C.L., Gu, W., and Accili, D. (2011). Proatherogenic abnormalities of lipid metabolism in SirT1 transgenic mice are mediated through Creb deacetylation. Cell Metab. *14*, 758–767.

Qin, W., Yang, T., Ho, L., Zhao, Z., Wang, J., Chen, L., Zhao, W., Thiyagarajan, M., MacGrogan, D., Rodgers, J.T., et al. (2006). Neuronal SIRT1 activation as a novel mechanism underlying the prevention of Alzheimer disease amyloid neuropathology by calorie restriction. J. Biol. Chem. *281*, 21745–21754.

Rafalski, V.A., and Brunet, A. (2011). Energy metabolism in adult neural stem cell fate. Prog. Neurobiol. *93*, 182–203.

Rafalski, V.A., Ho, P.P., Brett, J.O., Ucar, D., Dugas, J.C., Pollina, E.A., Chow, L.M., Ibrahim, A., Baker, S.J., Barres, B.A., et al. (2013). Expansion of oligodendrocyte progenitor cells following SIRT1 inactivation in the adult brain. Nat. Cell Biol. *15*, 614–624.

Renault, V.M., Rafalski, V.A., Morgan, A.A., Salih, D.A., Brett, J.O., Webb, A.E., Villeda, S.A., Thekkat, P.U., Guillerey, C., Denko, N.C., et al. (2009). FoxO3 regulates neural stem cell homeostasis. Cell Stem Cell *5*, 527–539.

Reynolds, B.A., and Weiss, S. (1992). Generation of neurons and astrocytes from isolated cells of the adult mammalian central nervous system. Science *255*, 1707–1710.

Riccio, A., Alvania, R.S., Lonze, B.E., Ramanan, N., Kim, T., Huang, Y., Dawson, T.M., Snyder, S.H., and Ginty, D.D. (2006). A nitric oxide signaling pathway controls CREB-mediated gene expression in neurons. Mol. Cell *21*, 283–294.

Saharan, S., Jhaveri, D.J., and Bartlett, P.F. (2013). SIRT1 regulates the neurogenic potential of neural precursors in the adult subventricular zone and hippocampus. J. Neurosci. Res. *91*, 642–659.

Tiberi, L., van den Ameele, J., Dimidschstein, J., Piccirilli, J., Gall, D., Herpoel, A., Bilheu, A., Bonnefont, J., Iacovino, M., Kyba, M., et al. (2012). BCL6 controls neurogenesis through Sirt1-dependent epigenetic repression of selective Notch targets. Nat. Neurosci. *15*, 1627–1635.

Vaquero, A., Scher, M., Lee, D., Erdjument-Bromage, H., Tempst, P., and Reinberg, D. (2004). Human SirT1 interacts with histone H1 and promotes formation of facultative heterochromatin. Mol. Cell *16*, 93–105.

Zhang, C.L., Zou, Y., He, W., Gage, F.H., and Evans, R.M. (2008). A role for adult TLX-positive neural stem cells in learning and behaviour. Nature *451*, 1004–1007.

Zhang, X., Odom, D.T., Koo, S.H., Conkright, M.D., Canettieri, G., Best, J., Chen, H., Jenner, R., Herbolsheimer, E., Jacobsen, E., et al. (2005). Genome-wide analysis of cAMP-response element binding protein occupancy, phosphorylation, and target gene activation in human tissues. Proc. Natl. Acad. Sci. USA *102*, 4459–4464.